AIAA-87-1879

A Simple Model for Finite Chemical Kinetics Analysis of Supersonic Turbulent Shear Layer Combustion

P. E. Dimotakis, and J. L. Hall
California Institute of
Technology, Pasadena, CA

AIAA/SAE/ASME/ASEE 23rd Joint Propulsion Conference

June 29-July 2, 1987/San Diego, California

A SIMPLE MODEL FOR FINITE CHEMICAL KINETICS ANALYSIS OF SUPERSONIC TURBULENT SHEAR LAYER COMBUSTION†

by,

Paul E. Dimotakis* and Jeffery L. Hall+

Graduate Aeronautical Laboratories
California Institute of Technology
Pasadena, California 91125

ABSTRACT

A simple flow/thermodynamic model is proposed to describe finite chemical kinetic rate combustion in a turbulent supersonic shear layer for the purposes of assessing Damköhler number effects in such flows. Sample calculations and comparisons for the $H_2/NO/F_2$ chemical system and the H_2/air system are described for a set of initial flow and thermodynamic conditions of the entrained reactants.

1. INTRODUCTION

The advent of supersonic chemical lasers and the resurgent interest in hypersonic flight has extended the range of flows for which estimates of the rate of molecular mixing and combustion are required to compressible high speed turbulent flows. In this flow environment, the chemical kinetics of fuel/oxidizer systems that are conventionally regarded as fast may find themselves in a regime where the rate of mixing, as dictated by the hydrodynamics, can overwhelm the rate of chemical product formation and associated heat release.

We can conceptually cast this discussion in terms of some characteristic fluid mechanical molecular mixing time (τ_m), and chemical reaction time (τ_χ), and their dimensionless ratio, i.e. the Damköhler number, defined by

$$Da = \frac{\tau_m}{\tau_\chi} . \qquad (1)$$

We note that in the limit of $Da \to \infty$ chemical production must be regarded as taking place in the strained diffusion layers (flame sheets) that are formed within the extent of the turbulent mixing region between the reactant-bearing fluids, which are entrained from each of the free streams; the lean entrained reactant does not have a chance to interdiffuse and homogenize on a molecular scale before it is has reacted. In that limit, therefore, the rate of chemical product formation is equal to the rate at which the lean reactant is diffusing (on a molecular scale) into fluid entrained from the other stream. In that case, the rate of chemical product formation will be dictated by the hydrodynamic entrainment and turbulent mixing processes and, in particular, will be independent of the chemical kinetics. On the other hand, we note that as the Damköhler number is decreased an increasing portion of the entrained fluids will have a chance to mix and homogenize on a molecular scale before the reactants in that portion have a chance to react. Finally, if the fluid mechanics may be treated as unaltered by variations in the chemical kinetic rate, it is evident that the chemical product formation and associated heat release attain their maximum in the limit of $Da \to \infty$. It is not possible to make any more product per unit time than the rate at which molecular diffusion of the reactants proceeds.

Efficient hypersonic propulsion requires that the associated turbulent combustion be realized in as high a Damköhler number regime as is feasible. For experiments in high Reynolds number and/or supersonic turbulence which attempt to estimate the extent of molecular mixing within the turbulent region, this is also an important regime; direct measurements of mixing, in view of the associated time and space scales, are generally out of the question. On the other hand, in a flow/kinetic rate regime in which the Damköhler number is sufficiently high, chemical reactions suggest themselves as the diagnostic probe of choice, since the heat release, or other associated chemical products, can serve as unambiguous markers for molecular mixing.

---

* Professor, Aero. & Appl. Phys. (member AIAA).

+ Graduate student, Aeronautics.

A model which first considered the relative effects of mixing rate and chemical kinetic rate was formulated by Broadwell (1974) in an attempt to analyze supersonic HF chemical laser performance. In that model, "the mixing is treated in an idealized way with the rate characterized by a single parameter, the angle at which the mixing zone spreads. The mixing, the chemical reactions, and lasing are allowed to occur simultaneously". By means of this model, a serious discrepancy between the premixed (constant mass) chemical reactor models (e.g. Emanuel & Whittier 1972), which were being used to analyze the supersonic shear layer chemical laser performance, and the observed dependence of the laser power on the cavity pressure was resolved.

An important addition to this idea was contributed by Konrad (1976) who concluded, on the basis of direct measurements of composition in (subsonic) shear layers, that the fluid carried in the free streams of a shear layer is entrained into the mixing region asymmetrically; for equal density free streams, the high speed stream is entrained preferentially. An explanation for this asymmetry, and a simple model for estimating the entrainment ratio E was proposed recently (Dimotakis 1986). These considerations suggested a zeroth order model for mixing in which the principal role of turbulence, following the initial stage of entrainment into the layer, is one resulting in a homogenization of the entrained fluids (and reactants) at a composition corresponding to the entrainment ratio E, i.e. to a high speed fluid mixture fraction ξ_E, given by

$$\xi_E = \frac{E}{E+1} \,. \qquad (2)$$

This simple picture was used by Konrad to account for the dependence of his composition fluctuations on the free stream density ratio. See figure 1.

Fluid that is mixed at the composition ξ_E of equation 2 plays an important role in the Broadwell & Breidenthal model (1982), in which the mixed fluid is partitioned as comprised of homogeneously mixed fluid at this composition and also as residing in strained diffusion layers. In this partition, the homogeneously mixed fluid volume fraction is regarded as a constant of the flow, and (for a given stoichiomentric mixture ratio) the volume fraction of the fluid residing in the flame sheets is assigned a volume fraction that is inversely proportional to the square root of the product of the flow Reynolds number and the fluid Schmidt number (this was the suggestion in the revised discussion of the model in Broadwell & Mungal 1986). This model was recently used by Broadwell & Mungal (1986) as the basis for their analysis of the experimental investigation of finite Damköhler number effects in a subsonic shear layer by Mungal & Frieler (1985). Broadwell & Mungal assumed that the rate of formation of the chemical product can be similarly partitioned as taking place within a homogeneously mixed fluid fraction and a flame sheet fluid fraction, where the assignement of these fractions is the same as the one made for the amount of chemical product in the original Broadwell & Breidenthal formulation.

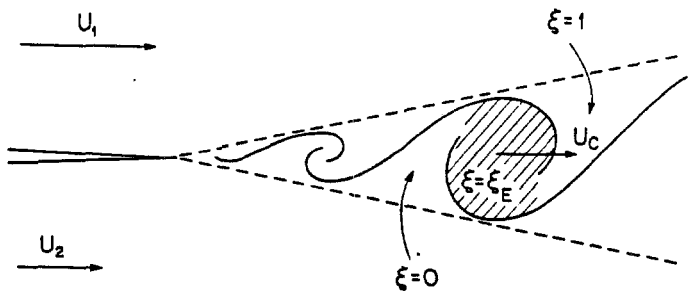

FIG. 1 Shear layer entrainment and growth.

We will not adopt the Broadwell-Mungal description of chemical product formation, primarily because it will serve our purposes to base the present discussion on an even simpler flow/thermodynamics model that will allow a realistic account of the chemical kinetics dynamics to be computed relatively readily.

2. THE PROPOSED MODEL

It is our purpose in this discussion to explore the interrelation between the rate of entrainment and mixing, and finite chemical kinetics in high Reynolds number shear layers, extending to supersonic flow. We will attempt to do this in the simplest terms that capture the salient features of this behavior, using two fuel/oxidizer systems as examples: the $H_2/NO/F_2$ system and the H_2/air system. While some of our results will be peculiar to these two systems, many of the conclusions are general and we would like to hope that the adopted simple formulation and implementation can serve as a useful guide.

The proposed scheme has three main components:

1. the entrainment/mixing model,

2. the thermodynamic model,

and

3. a chemical kinetic model.

2.1 Entrainment/mixing formulation

We will adopt the simple idea suggested by Konrad (1976), namely the one which views the molecularly mixed fluid in the shear layer as homogenized at a single-valued composition dictated by the entrainment ratio E (cf. equation 2). The entrainment ratio E will, in turn, be computed using the simple ideas discussed by Dimotakis (1986). Briefly, it was argued in that discussion that the (volumetric) entrainment ratio should be approximated by

$$E = \frac{U_1 - U_c}{U_c - U_2} \left(1 + \frac{\ell}{x}\right) , \qquad (3)$$

where $U_{1,2}$ are the high and low speed shear layer free stream velocities respectively, U_c is the convection velocity of the large structures in the layer, and ℓ/x is the large structure spacing to position ratio.

For subsonic flow, the convection velocity can be estimated by applying the Bernoulli equation in the large structure convection frame, in which it should (approximately) apply on the streamlines through the stagnation points in between the vortices. This yields (for equal free stream static pressures),

$$\rho_1 (U_1 - U_c)^2 = \rho_2 (U_c - U_2)^2,$$

or,

$$\frac{U_1 - U_c}{U_c - U_2} = \left(\frac{\rho_1}{\rho_2}\right)^{1/2} . \qquad (4)$$

The large structure spacing to position ratio ℓ/x is found (empirically) to be independent of the density ratio and approximately given by

$$\frac{\ell}{x} = 0.68 \frac{1 - U_2/U_1}{1 + U_2/U_1} . \qquad (5)$$

Combining these results, one then obtains an estimate for the volumetric entrainment ratio for subsonic flow given by

$$E = \left(\frac{\rho_1}{\rho_2}\right)^{1/2} \left(1 + 0.68 \frac{1 - U_2/U_1}{1 + U_2/U_1}\right) . \qquad (6)$$

For supersonic flow, the convection velocity can be approximated using the isentropic relations connecting the stagnation pressure (in the vortex convection frame) and the static pressure in each of the free streams, which for equal free stream static pressures yields the implicit relation

$$\left(1 + \frac{\gamma_1 - 1}{2} M_{c1}^2\right)^{\gamma_1/(\gamma_1 - 1)} = \left(1 + \frac{\gamma_2 - 1}{2} M_{c2}^2\right)^{\gamma_2/(\gamma_2 - 1)} , \qquad (7)$$

where $\gamma_{1,2}$ are the ratios of specific heats in each of the free streams and

$$M_{c1} = \frac{U_1 - U_c}{a_1} , \qquad M_{c2} = \frac{U_c - U_2}{a_2} , \qquad (8)$$

are the convective Mach numbers, with $a_{1,2}$ the speeds of sound in the high and low speed free streams respectively. This relation was proposed by Bogdanoff (1983) on the basis of a different set of arguments. We note here that for low to moderate supersonic free stream Mach numbers $M_{1,2}$, the convective Mach numbers will not be too high and the incompressible relation (equation 4) may serve as an adequate approximation.

While there is insufficient information to establish a reliable relation for ℓ/x for supersonic flow, it is a probably a fair guess that ℓ/x will continue to be scaled by the shear layer growth rate δ/x. Additionally, it is known (Papamoschou 1986) that a supersonic shear layer at the same velocity and density ratio will, for high values of the convective Mach number, grow considerably slower (by a factor of approximately 5) than its incompressible counterpart. This suggests that, at high convective Mach numbers, ℓ/x may be estimated by

$$(\ell/x)_{M_{c1} > .5} = 0.2 \, (\ell/x)_{M_{c1} < .25} , \qquad (9)$$

where ℓ/x at low convective Mach numbers ($M_{c1} < .25$) can be estimated using equation 5. Accordingly, the second factor $(1 + \ell/x)$ in the basic relationn for the entrainment ratio (equation 3) will be much closer to unity for (high) supersonic flow ($M_{c1} \geq 0.5$) than for subsonic flow.

We can visualize the mixing process, in this picture, as the flow through two streamtubes (generally of unequal cross-section), with inlet

velocities $U_1 - U_c$ and $U_c - U_2$ respectively, filling the molecularly mixed fluid balloon (at constant pressure) with a mole rate that is the sum of the two entrainment contributions from each of the free streams. The total number of moles $n_T(t)$ in the balloon, at any one time $t = x/U_c$ represents the total number of moles of molecularly mixed fluid in the layer, corresponding to a mixed fluid thickness δ_m. This is smaller than the total shear layer thickness δ, to the extent that only a (mole) fraction δ_m/δ of the fluid within the shear layer wedge boundaries is mixed on a molecular scale. The ratio of the two entrainment feed rates $\dot{n}_{1,e}$ and $\dot{n}_{2,e}$ are then computed in accord with the entrainment ratio while the total feed rate is such as to yield the correct value of $\delta_m(t)$, at each station $x = t\,U_c$. See figure 2.

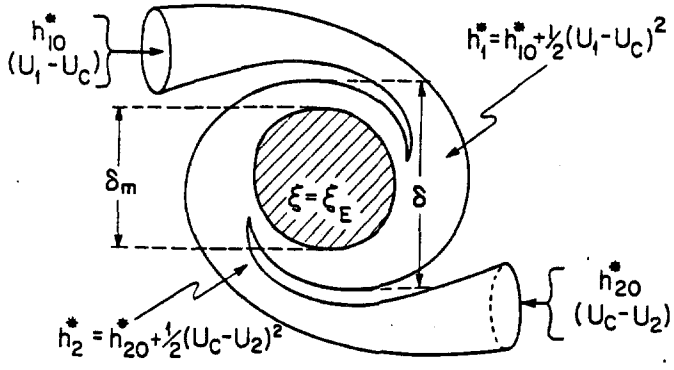

FIG. 2 Convective frame entrainment/mixing schematic.

The species composition in each of the free streams is specified via the mole fractions X_{α_i} of the species α carried by the i-th stream. This yields an entrainment feed rate for the species α from each of the free streams, given by

$$\dot{n}_{\alpha_i} = X_{\alpha_i}\,\dot{n}_{i,e}\,, \quad i = 1,2\,. \tag{10}$$

The contents of the balloon are regarded as homogeneously mixed at all times, the respective feed rates guaranteeing the correct composition (equation 2) thereby. That neighboring balloons (large scale structures) coalesce from time to time to produce larger balloons of the same composition does not alter this picture as far as the chemical dynamics are concerned.

Before leaving the discussion of the entrainment/mixing component of the model, we should note that an important ingredient of the turbulent mixing process is ignored by this simple picture. It is the effect of the rapid increase in the rate of strain experienced by a particular segment of the strained reactant interface between the two entrained fluids, as it cascades in its Lagrangian frame to the smallest scales at which it ultimately homogenizes on a molecular scale. Ignoring this effect will result in an overestimation of the effective chemical kinetic rate, as we will discuss below.

2.2 Thermodynamics formulation

To compute the chemical kinetics of the system, we need to keep track of the temperature evolution in the homogeneous reactor. In particular, in addition to the heat released in the chemical reactions, we need to estimate the enthalpy flux which the entrained fluids contribute to the total enthalpy of the contents of the balloon. This will be computed by assuming that the entrained fluids are approximately brought to rest in the balloon (large scale) convection frame adiabatically. This yields an estimate for the stagnation enthalpy contributed in this frame from each of the free streams given by

$$h^*_{i,e} = h^*_{i,0} + \frac{1}{2}(U_i - U_c)^2\,,$$

where $i = 1,2$ corresponds to the high and low speed streams respectively, $h^*_{i,e}$ is the resulting specific stagnation enthalpy (J/kg) contributed by the i-th stream in the convection frame and $h^*_{i,0}$ is the specific (static) enthalpy of the i-th free stream. It will be convenient to express quantities in molar form for the chemical calculations below. Accordingly, we have for the molar enthalpy (J/kmole) of each stream

$$h_{i,e} = h_{i,0} + \frac{1}{2}\langle W\rangle_i\,(U_i - U_c)^2\,, \tag{11}$$

where $\langle W\rangle_i$ is the (mean) molecular weight of the i-th stream.

Assuming that the balloon can be treated as an adiabatic system and that the kinetic energy of the internal motion (in the balloon convection frame) is negligible†, we obtain the energy equation (at constant pressure)

$$\dot{H}_T = \dot{H}_e = \dot{n}_{1,e}\,h_{1,e} + \dot{n}_{2,e}\,h_{2,e}\,. \tag{12}$$

† The latter assumption may have to be revised at very high convective Mach numbers.

where H_T is the total enthalpy of the contents of the balloon. Chemical reactions and combustion notwithstanding, the total enthalpy changes only as a consequence of the entrainment contribution.

The total enthalpy of the system is also expressible (for an ideal gas) as the sum of the molar contributions. Differentiating with respect to time, we have

$$\dot{H}_T = \sum_\alpha (\dot{n}_\alpha h_\alpha + n_\alpha \dot{h}_\alpha) .$$

We can use the relation $\dot{h}_\alpha = c_{p\alpha}\dot{T}$, where $c_{p\alpha}$ is the molar heat capacity at constant pressure of the α species and T is the balloon temperature, and combine with equation 12 to obtain the temperature evolution equation (at constant pressure), i.e.

$$C_p \dot{T} = \dot{H}_e - \sum_\alpha \dot{n}_\alpha h_\alpha , \qquad (13)$$

where C_p is the total heat capacity of the system contents at constant pressure and $\dot{n}_\alpha$ is the total rate of change of the number of moles of the α species (sum of entrainment feeds plus chemistry), i.e.

$$\dot{n}_\alpha = \dot{n}_{\alpha_1} + \dot{n}_{\alpha_2} + \dot{n}_{\alpha_\chi} . \qquad (14)$$

2.3 Chemical kinetics formulation

The chemical kinetics calculations are realized using the CHEMKIN (Kee et al 1980) code package. In particular, borrowing from their description, we have for the j-th chemical equation

$$\sum_\alpha a_{\alpha_j} \chi_\alpha \; \updownarrow \; \sum_\alpha b_{\alpha_j} \chi_\alpha , \qquad (15)$$

where the a_{α_j} and b_{α_j} are the (integer) stoichiometric coefficients and χ_α is the chemical symbol of the α species. The production rate [kmoles/(m^3·sec)] for the species α is then computed as the sum over all the chemical reactions, i.e.

$$\dot{\omega}_\alpha = \sum_j (b_{\alpha_j} - a_{\alpha_j}) q_j , \qquad (16)$$

where q_j is the rate of progress variable for the j-th chemical reaction, computed as the difference between the forward and reverse rates. For a two-body chemical reaction, this is given by

$$q_j^{(2)} = k_{f,j} \prod_\alpha [\alpha]^{a\alpha j} - k_{r,j} \prod_\alpha [\alpha]^{b\alpha j} , \qquad (17a)$$

where $[\alpha] = n_\alpha / V$ is the molar concentration of the α species with $V = V(t)$ the balloon volume, and $k_{f,j}$ and $k_{r,j}$ are the forward and reverse rate constants for the j-th reaction. For a three-body chemical reaction the rate of progress variable is computed as

$$q_j^{(3)} = (\sum_\alpha n_{\alpha_j} [\alpha]) \, q_j^{(2)} , \qquad (17b)$$

where if all species contribute equally to the reaction (e.g. any third body M in the vernacular) the efficiency coefficients n_{α_j} are all equal to unity and the first factor in the expression for $q_j^{(3)}$ is given by (ideal gas law)

$$\sum_\alpha n_{\alpha_j} [\alpha] = \sum_\alpha [\alpha] = \frac{n_T}{V} = \frac{p}{RT} . \qquad (18)$$

The forward rate constants are computed assuming an Arrhenius temperature dependence form, i.e.

$$k_{f,j}(T) = A_j \, T^{\beta j} \exp(-\frac{E_j}{RT}) , \qquad (19)$$

while the reverse rate constants $k_{r,j}$ are related to the forward rate constants through the equilibrium constants of the j-th reaction. The coefficients A_j, β_j and E_j, as well as any non-unity three-body efficiency coefficients n_{α_j}, must be specified for each chemical reaction j.

Using equation 16 for the species production rate, we then compute the chemical rate of change of the number of moles of the species α as needed in equation 14, using the relation

$$\frac{1}{V(t)} \dot{n}_{\alpha\chi}(t) = \dot{\omega}_\alpha(t) \qquad (20)$$

where V(t) is the volume of the balloon, computed in turn using the ideal gas law equation of state, i.e.

$$V(t) = n_T(t) \frac{RT(t)}{p} , \quad n_T(t) = \sum_\alpha n_\alpha(t) . \qquad (21)$$

The chemical reactions describing the $H_2/NO/F_2$ system are listed in the appendix, with the Arrhenius coefficients for each reaction j. The H_2/air system was used as documented in Smooke et al (1983). By way of example, if a particular species A is entrained as part of the high speed fluid with a mole fraction X_{A_1} and as part of the

low speed fluid with a mole fraction X_{A_2}, and participates in a (say, j = 1) chemical reaction

$$A + B \rightleftarrows C + D$$

its evolution equation would be given by (note that $a_{A_1} = a_{B_2} = 1$, in this case)

$$\frac{1}{V}\dot{n}_A = \frac{1}{V}\left(X_{A_1}\dot{n}_1 + X_{A_2}\dot{n}_2 \right) - k_{f,1}\left(\frac{n_A}{V}\right)\left(\frac{n_B}{V}\right) + \ldots \qquad (22)$$

The manner in which the volume V = V(t) enters on the left hand side is, perhaps, noteworthy.

2.4 Model implementation

Having specified the entrainment/mixing infusion history $\dot{n}_1(t)$ and $\dot{n}_2(t)$, the temporal evolution of the flow/chemical system can be computed in the convective frame (which we can transform to the fixed shear layer combustor frame via the convective velocity, i.e. $x = t\,U_c$).

For an arbitrary history $\dot{n}_1(t)$ and $\dot{n}_2(t)$, the resulting non-linear system of equations is sufficiently complex to render drawing of general conclusions difficult. While such an arbitrary case can readily be studied numerically, it is possible to gain valuable insight by restricting the discussion to constant $\dot{n}_1$ and $\dot{n}_2$, as appropriate anyway to turbulent shear layers beyond the mixing transition (Bernal et al 1979). Additionally, in the model, we will allow the balloon reactor to be precharged with an initial amount and composition of reactants and at an initial thermodynamic state (temperature T_0) comnputed by assuming that while the entrainment has proceeded starting from t = 0, the chemistry is not initiated until a time $t = t_0 = x_0 / U_c$.

The latter provision should be a useful approximate description in the case of hypergolic (or near-hypergolic) reactants that have been entrained (but not as yet mixed) and which are mixed on a molecular scale rather abruptly as they move through the mixing transition at $x_0 = x_{tr}$, or, in the case of non-hypergolic reactants (for the flow conditions) that are allowed to mix and are ignited (by some external means) at some convective time $t_0 = t_{ig} = x_{ig} / U_c$. This is equivalent to an entrainment/mixing infusion history given by

$$\int_0^t \dot{n}_i(t')\,dt' = \begin{cases} 0, & t < t_0, \\ t\,\dot{n}_{i_\infty}, & t > t_0, \end{cases} \qquad (23)$$

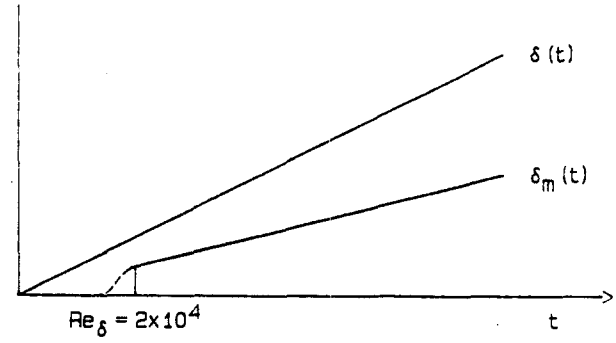

FIG. 3 Shear layer total and mixed fluid thickness.

where $\dot{n}_{i_\infty}$ corresponds to the constant entrainment/mixing infusion rate from the i-th stream, far downstream from the transition/ignition region. This situation is depicted in figure 3, and is reflected in the growing total shear layer thickness $\delta(t)$, corresponding to the constant rate (per unit time in the convective frame) at which fluid is entrained (inducted) into the layer, and $\delta_m(t)$ corresponding to the constant infusion (contribution per unit time to the mixed fluid) flux the resulting balloon reactor (molecularly mixed fluid) volume V(t). In this picture, the balloon volume V(t), per unit span of shear layer, is to be viewed as the product of a fixed streamwise thickness dx and the mixed fluid thickness $\delta_m(t)$.

Finally, we note that implicit in this discussion is the assumption that the effects of heat release on the fluid dynamics are small. In the context of the present model, the relevant question is the effect of the heat release on the entrainment ratio. At least for subsonic flow, this issue was specifically addressed in the work documented in Hermanson (1985) and Hermanson et al (1987). Based on the conclusions drawn from that work, one could certainly provide corrected estimates for $\dot{n}_1$ and $\dot{n}_2$ as a function of heat release. On the other hand, the main conclusion in that discussion was that these effects are small and would therefore be unwarranted by, and inconsistent with the spirit of the simple flow/mixing model proposed here.

3. RESULTS and DISCUSSION

3.1 General properties

Assuming that the entrainment/mixing flux $\dot{n}_i$ from the i-th stream is as described in the preceding section, we may draw the following useful conclusions.

Provided it ignites and that the entrained reactants do not quench the reaction, the system (balloon reactor contents) reaches a final equilibrium temperature T_f which is equal to the adiabatic flame temperature of a constant mass reactor at chemical equilibrium, corresponding to an atomic composition dictated by the entrainment/mixing flux ratio E. As a corollary, we have $\dot{V}$ = constant and therefore V(t) ~ t at equilibrium, since $\dot{n}_T$ = constant, p = constant, and, in the limit, T = constant.

The second important conclusion is that if the lean (or rate-limiting) reactant is entrained from, say, the high speed stream (stream 1), the evolution of the system is a function of a single dimensionless parameter

$$\Omega_1 = \frac{\dot{n}_1 \tau_\chi}{n_1(t_0^+)} , \qquad (24)$$

where $n_1(t_0^+)$ is the (precharge) number of stream 1 moles at $t = t_0^+$, $\dot{n}_1$ is the (constant) entrainment/mixing rate from stream 1, and τ_χ is the characteristic chemical time, defined here as the maximum slope thickness intercept of the T(t) curve with the $T = T_f$ line for a constant mass reactor, as will be illustrated below. In particular, for $\Omega \ll 1$, as we would expect, the system evolution is the same as that of a constant mass reactor, since the asymptotic temperature rise will be realized before any substantial amounts of entrained reacts have been added. In the opposite limit of $\Omega \gg 1$, however, the important and perhaps surprising conclusion is that not only the final equilibrium state but also the system evolution is independent of the entrainment/mixing rate $\dot{n}_1$. This behavior is depicted in figure 4, in which the scaled temperature rise in the mixed fluid reactor, i.e.

$$\frac{\Delta T(t)}{\Delta T_f} = \frac{T(t) - T_0}{T_f - T_0} , \qquad (25)$$

is plotted as a function of time, for a typical low heat release $H_2/NO/F_2$ reactant/diluent combination as used in the Mungal & Dimotakis (1984) data and in the Mungal & Frieler 1985 Damköhler number study. The solid curve corresponds to the evolution of a constant mass ($\Omega = 0$) reactor. The dashed line is the maximum slope extrapolation of that curve, used to compute the intercept with $\Delta T(t)/\Delta T_f = 1$ at the time $t = \tau_\chi$. Finally, the dot-dashed curve depicts the asymptotic, entrainment-dominated reactor (computed using a value of $\Omega = 100$). The behavior in the latter case is asymptotic in the sense that additional increases in Ω would not discernibly alter the resulting $\Delta T(t)/\Delta T_f$ curve.

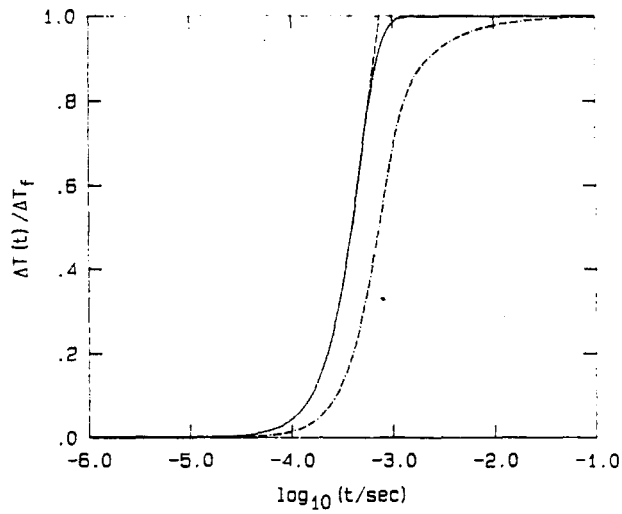

FIG. 4 Constant mass (solid line) vs. entrainment-dominated (dot-dashed line) mixed fluid reactor behavior.

3.2 Using the model

We will demonstrate the use of the proposed model by attempting a calculation of the Mungal & Frieler (1985) Damköhler number study data. In that experiment, the effective rate of reaction of the $H_2/F_2/NO$ system in the mixing zone was controlled by varying the concentration (mole fraction) of NO that was premixed with H_2 in the high speed stream. The experiments were conducted in the shear layer facility described in Mungal & Dimotakis (1984), with a free stream velocity ratio of $U_2/U_1 = 0.4$ and a density ratio $\rho_2/\rho_1 = 1$. The high speed stream was comprised of (mole fractions) 8% H_2, a nominal mole fraction of NO of $[NO]_* = 0.03\%$, and the rest N_2 at room temperature. The low speed stream was composed of 1% F_2 and 99% N_2, also at room temperature.

The H_2/F_2 reaction requires free F atoms, which under these conditions are produced via the $NO + F_2 \rightarrow NOF + F$ reaction (see Appendix A). The

kinetic rate can be reduced to zero in the absence of any free F atoms, a situation that is realized (under these conditions) if there is no premixed NO in the H_2 bearing stream. Accordingly, the kinetic rate controlling parameter in the experiments was the concentration of the premixed NO, that the authors cited normalized by the nominal concentration $[NO]_* = 0.03\%$. In particular, experiments were conducted at $[NO]/[NO]_* = 1/32$, 1/23, 1/16, 1/8, 1/4, 1/2, 1, 3/2 and 2 at the lower velocity runs ($U_1 = 22$ m/s), and at $[NO]/[NO]_* = 1/16$, 1/4, 1 and 2 at the higher Reynolds number run ($U_1 = 44$ m/s).

The experimental uncertainty in determining the amount of [NO] is estimated to be of the order of $0.03\,[NO]_*$ (laboratory record, G. Mungal private communication). The experimental uncertainty in the total amount of product, computed in those measurements as the volume fraction $\delta_p([NO])/\delta$ in the layer occupied by chemical product, was estimated to be of the order of 3% to 5%.

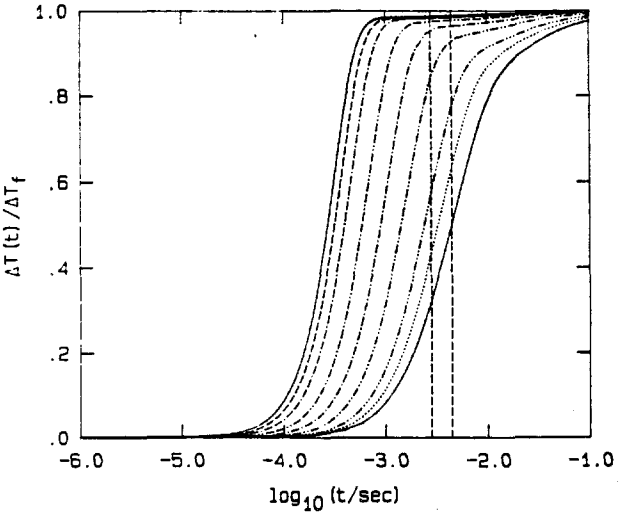

FIG. 5 $\Delta T(t)/\Delta T_f$ computed for Mungal & Frieler (1985) data. Curves from left to right for $[NO]/[NO]_*$ of 2, 3/2, 1, 1/2, 1/4, 1/8, 1/16, 1/23, 1/32. Vertical dashed lines for (scaled) times $t' = 2.75$ ms, 4.4 ms respectively (see text below).

The fact that the Reynolds number is different in the two sets of runs has, of course, no effect on the shape of the model $\Delta T(t)/\Delta T_f$ curves. Since other parameters were kept fixed, these curves are only a function of the $[NO]/[NO]_*$ ratio for these experiments. The results of the computations corresponding to the experimental conditions are plotted in figure 5 along with the Mungal & Frieler data and their experimental error bars.

The dependence of the chemical product δ_p/δ volume fraction on the $[NO]/[NO]_*$ ratio for the two Reynolds number runs is read off such a family of curves at a fixed Lagrangian time, which is different for each Reynolds number case. The reactor is precharged to the amount and composition corresponding to the conditions at the end of the mixing transition region, as described in section 2.4. The experimental Lagrangian time is given by

$$t = \frac{x - x_0}{U_c} , \qquad (26)$$

where x is the location of the fixed measuring station (= 45.7 cm), x_0 is taken to be at the end of the mixing transition (hypergolic reactants) at $\Delta U \cdot \delta/\nu \approx 2\times10^4$ (as recommended by Mungal & Frieler 1985), and U_c is the convection velocity. This yields estimates for the experimental Lagrangian time at the measuring station of $t = 20.8$ ms and $t = 13.1$ ms for the low and high Reynolds number experiments respectively.

In using the model to estimate the experimental data, we note that the reaction rate coefficients for the $H_2/NO/F_2$ system are better known than most rate coefficients. In particular, for that system they are known to within a factor of 3, or so. While it is not possible to make general statements without a specific sensitivity analysis, a qualitative estimate of the global effect of such an uncertainty on the calculated quantities can be made for the entrainment-dominated reactor ($\Omega \gg 1$) as follows. A rescaling of the reaction rate coefficients by a dimensionless scaling factor κ, i.e. $k'_{f,j} \rightarrow \kappa k_{f,j}$, produces the same chemical evolution as the unscaled coefficients did at a (scaled) time $t' = t/\kappa$.

There is an other, possibly more important, effect we have ignored that may have similar time-scaling consequences, namely the unsteady evolution of the rate of strain σ that is imposed by the turbulent field on the interface between the two interdiffusing fluids. In solving the unsteady diffusion problem, one can show that for times that are large compared to the reciprocal of the strain rate, i.e. for $t \gg 1/\sigma$, the solution to the unsteady diffusion problem in the presence of an imposed strain rate, tends asymptotically to those of the unsteady diffusion problem in the absence of an externally imposed strain rate, evaluated at a time $t = 1/\sigma$ (Carrier, Fendel & Marble 1975, Marble & Broadwell 1977, Dimotakis 1987). Accordingly, instead of interpreting the corresponding solutions as functions of the product of an effective kinetic rate k_* and time, i.e. $k_* t$, they should be interpreted as functions of the ratio k_*/σ. For a

two dimensional shear layer, the strain rates are scaled by $\Delta U/\delta$ and therefore $1/\sigma \sim \delta/\Delta U \sim t$. We should also mention that Broadwell & Mungal (1986), who provided an approximate solution for a finite kinetic rate analysis of a strained flame sheet using a control volume approach, also found that the solution dependence on the kinetic rate and rate of strain is via the group k_*/σ. Since the predominant fraction of molecularly mixed fluid is associated with the smallest scales of the turbulent flow, where not only the rate of strain σ is high but also the rate at which it, in turn, increases with Lagrangian time for each fluid element ($\dot{\sigma}$) is high, this effect is potentially important.

For both of these reasons we will accept an undetermined time scaling factor κ as an adjustable parameter. Uncertainties in the kinetic rate coefficients aside a more realistic hydrodynamic account of the turbulent entrainment/mixing process would hopefully remove the need for such an adjustment. We note here, however, that this is quite an aside, as many important kinetic rate coefficients are often uncertain by factors in excess of an order of magnitude.

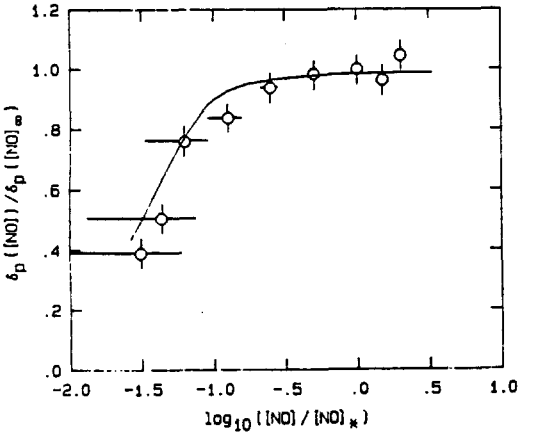

Fig. 6a

The resulting computations are depicted in figures 6a and 6b, for the low and high Reynolds number runs respectively. The value of the time scaling factor used to compute these curves was $\kappa = 5$. The resulting (scaled) Lagrangian times t' corresponding to the two sets of data (t' = 4.4 ms, 2.75 ms, respectively) are indicated by the vertical dashed lines in figure 5.

Discounting for the need of the time-scaling factor κ, we see that the salient features of the data are captured correctly, especially considering the simplicity of the hydrodynamics description.

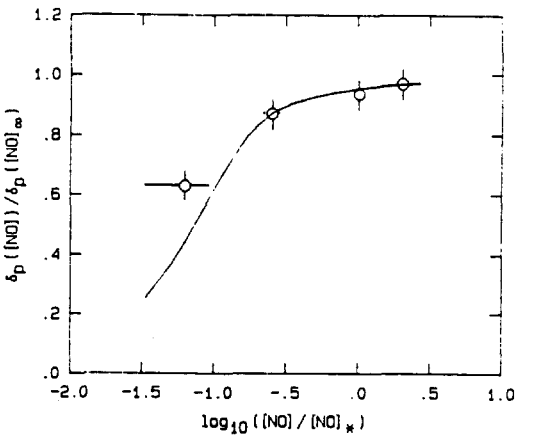

(b)

FIG. 6 $\delta_p([NO])/\delta p([NO]*)$ for Mungal & Frieler (1985) data. (a) low Reynolds number data ($U_1 \approx 22$ m/s), (b) high Reynolds number data ($U_1 \approx 44$ m/s.

3.3 Supersonic $H_2/NO/F_2$ system calculations

Sample calculations at 1 Atm pressure for a supersonic high speed stream bearing H_2, NO and N_2 at $M_1 \approx 3.0$, and a subsonic low speed stream bearing F_2 and N_2 at $M_2 \approx 0.3$ and a stagnation temperature of 300 K were performed. The $\Delta T(t)/\Delta T_f$ evolution of the system is depicted in figure 7 for high speed stream stagnation temperatures of 300 K and 600 K at low reactant concetrations. Note that the difference in the final temperature rise ΔT_f in the two cases is due to the difference in the entrainment ratio. The increase in the effective chemical kinetic rate is manifest.

A study of an additional increase in the effective rate was undertaken by raising the reactant concentrations in both streams, keeping the stagnation temperatures for the high and low speed streams at 600 K and 300 K, respectively. The resulting calculations are depicted in figure 8.

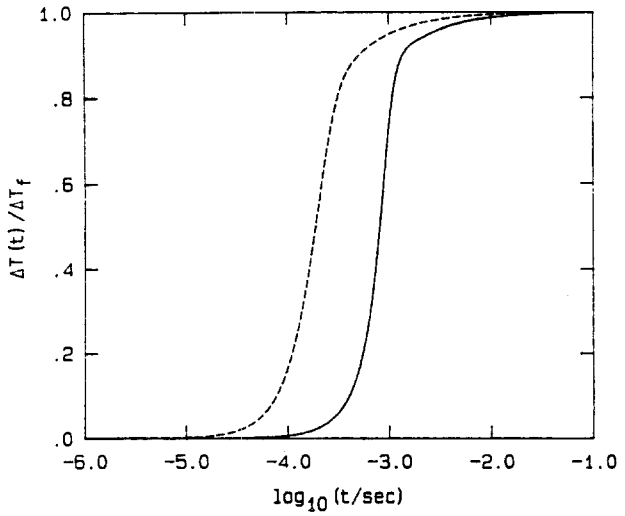

FIG. 7 $\Delta T(t)/\Delta T_f$ computed at 1 Atm (static) pressure, for a 2% H_2 / 0.1% NO / 97.9% N_2 M_1 = 3.0 stream, and a 2% F_2 / 98% N_2 stream at M_2 = 0.3 and a stagnation temperature of 300 K. Solid line and dashed line for a high speed stagnation temperature of 300 K (ΔT_f = 128 K) and 600 K (ΔT_f = 158 K) respectively.

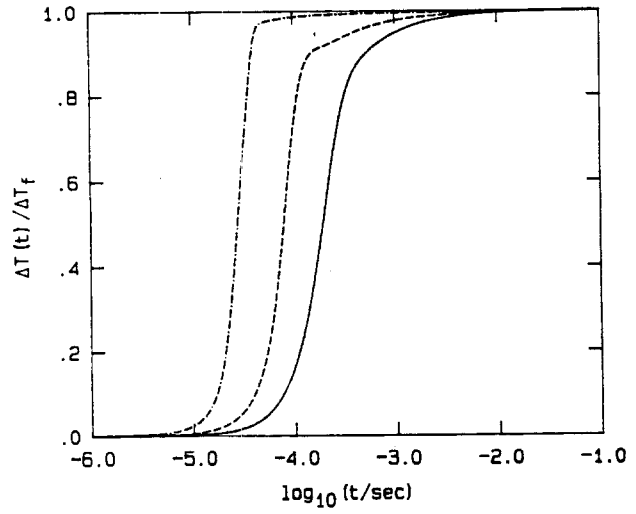

FIG. 8 $\Delta T(t)/\Delta T_f$ computed at 1 Atm (static) pressure, for a H_2/0.1%NO/N_2 stream at M_1 = 3.0 and a stagnation temperature of 600 K, and a F_2/N_2 stream at M_2 = 0.3 and a stagnation temperature of 300 K. Solid line for 2%H_2 and 2%F_2 (ΔT_f = 158 K), dashed line for 6%H_2 and 6%F_2 (ΔT_f = 459 K), dot-dashed line for 20%H_2 and 20%F_2 (ΔT_f = 1,353 K).

As can be ascertained from these calculations, characteristic chemical reaction times in the range of 10 μs to 1 ms can be attained by such means.

3.4 Supersonic H_2/air system calculations

Calculations using the H_2/air chemical system, with flow conditions for a hypothetical hypersonic vehicle are described below. It is assumed that the H_2 bearing stream has been preheated to 1,500 K, as it is utilized as a coolant, and additionally heated in a precombustion chamber using a portion of the inlet air, as required to reach a stagnation temperature of 2,200 K. It is subsequently discharged in the primary combustor at M_2 = 1.25 to form the low speed stream of a supersonic shear layer. The high speed stream is assumed to be air at a Mach number M_1 equal to 1/3 of the flight Mach number M_∞ and at a stagnation enthalpy corresponding to a static temperature of 300 K at M_∞.

Figure 9 depicts the resulting absolute temperature T(t) calculations, for a flight Mach number of M_∞ = 12 and (static) pressures in the shear layer combustion chamber of 0.75, 0.5 and 0.25 Atm. Note that whereas the reactants ignite increasingly rapidly as the pressure is raised, equilibrium is attained extremely slowly, as a consequence of energetic minor species which in turn reach their equilibrium concentrations extremely slowly (3 time decades), independently of the pressure at these conditions.

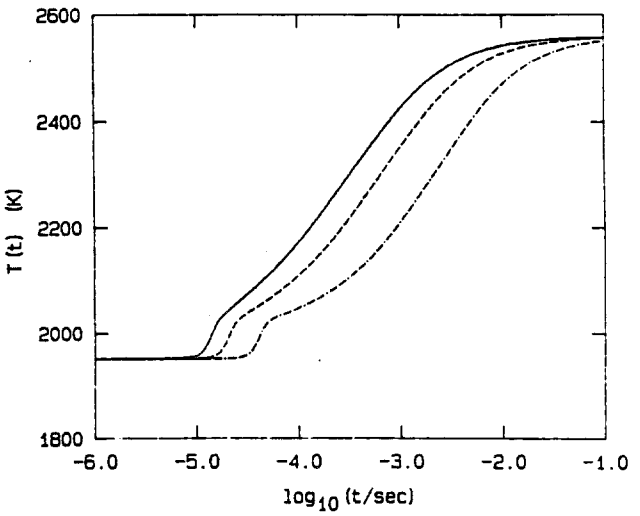

FIG. 9 T(t) computations for a hypothetical hypersonic flight vehicle at M_∞ = 12, for p = 0.75 Atm (solid line), p = 0.5 Atm (dashed line) and p = 0.25 Atm (dot-dashed line).

Calculations were also performed at a fixed static pressure of 0.5 Atm to illustrate the effect of flight Mach number M_∞. It is important to note that the main consequence of increasing M_∞ is the attendant increase in the initial mixture

temperature (T_0 in the notation of section 2.4).

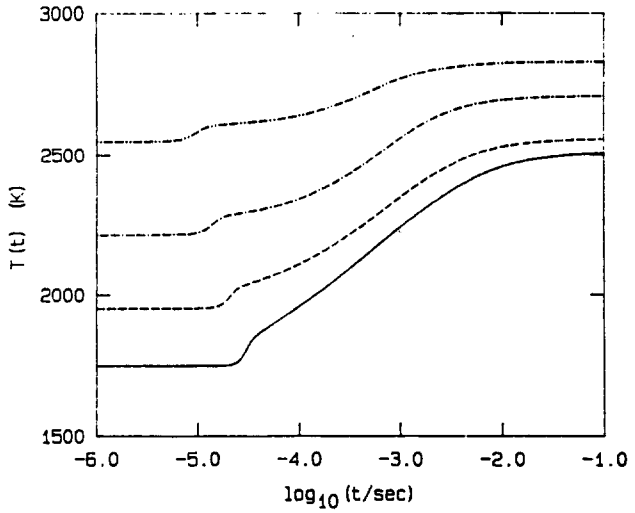

FIG. 10 T(t) computations for a hypothetical hypersonic flight vehicle at a static pressure of 0.5 Atm. Solid line for $M_\infty = 9$, dashed line for $M_\infty = 12$, dot-dashed line for $M_\infty = 15$ and dot-dot-dashed line for $M_\infty = 18$.

The conspicuous decrease in the equilibrium temperature rise ΔT_f is a consequence of the increasing participation in the final equilibrium population of energetic species, which under these conditions of increasing absolute temperature cannot really be considered as minor.

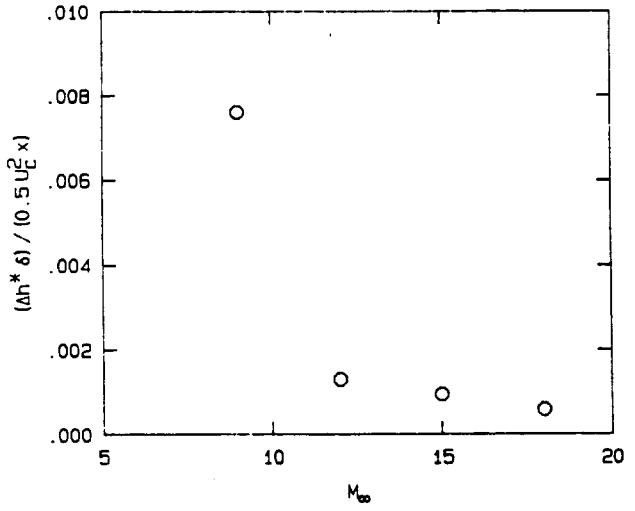

FIG. 11 Normalized specific enthalpy coefficient for hypothetical hypersonic shear layer combustor contribution.

In an effort to assess the relative contribution of the shear layer combustion to the overall enthalpy release, we have estimated the coefficient $2\Delta h^*/U_c^2$ of the specific enthalpy release at the end of a 1 meter shear layer combustor, multiplied by the estimated shear layer thickness δ/x, as computed from the data in figure 10. The results are depicted in figure 11. Note that the rapid decrease from $M_\infty = 9$ to $M_\infty = 12$ is a consequence of the transition of the δ/x growth rate to the supersonic regime ($M_{c_1} > 0.5$).

4. ACKNOWLEDGEMENTS

We would like to acknowledge the helpful discussions with Dr. G. Mungal. The work was supported by AFOSR Grant No. 83-0213.

5. REFERENCES

BAULCH, D. L., DUXBURY, J., GRANT, S. J., MONTAGUE, D. C. [1981] "Evaluated kinetic data for High Temperature Reactions", vol. 4, published in J. Phys. Chem. Ref. Data 10, Suppl. 1.

BERNAL, L. P., BREIDENTHAL, R. E., BROWN, G. L., KONRAD, J. H. and ROSHKO, A. [1979] "On the Development of Three Dimensional Small Scales in Turbulent Mixing Layers.", 2nd Symposium on Turbulent Shear Flows, 2-4 July 1979, Imperial College, England.

BOGDANOFF, D. W. [1983] "Compressibility Effects in Turbulent Shear Layers (TN)", AIAA J. 21(6), 926 - 927.

BROADWELL, J. E. [1974] "Effect of Mixing Rate on HF Chemical Laser Performance", Applied Optics 13, 962-967.

BROADWELL, J. E. and BREIDENTHAL, R. E. [1982] "A Simple Model of Mixing and Chemical Reaction in a Turbulent Shear Layer", J. Fluid Mech. 125, 397-410.

BROADWELL, J. E. and MUNGAL, M. G. [1986] "The effects of Damköhler number in a turbulent shear layer", GALCIT Report FM86-01.

CARRIER, G. F., FENDELL, F. E. and MARBLE, F. E. [1975] "The Effect of Strain on Diffusion Flames", SIAM J. Appl. Math. 28(2), 463-500.

COHEN, N. and BOTT, J. F. [1982] "Review of rate Data for reactions of Interest in HF and DF lasers", The Aerospace Corporation, report SD-TR-82-86.

DIMOTAKIS, P. E. [1986] "Two-Dimensional Shear-Layer Entrainment", AIAA J. 24(11), 1791-1796.

DIMOTAKIS, P. E. [1987] "Turbulent shear layer mixing with fast chemical reactions", US-France Workshop on Turbulent Reactive Flows, 7-10 July 1987 (Rouen, France), 9.1-106 (GALCIT Report FM87-01).

EMANUEL, G. and WHITTIER, J. S. [1972] "Closed-Form Solution to Rate Equations for an F + H_2 Laser Oscillator", Appl. Optics 11(9), 2047-2056.

KEE, R. J., MILLER, J. A., and JEFFERSON, T. H. [1980] "CHEMKIN: A General Purpose, Problem-independent, Transportable, Fortran Chemical Kinetics Code Package", SANDIA Report SAND80-8003.

KONRAD, J. H. [1976] An Experimental Investigation of Mixing in Two-Dimensional Turbulent Shear Flows with Applications to Diffusion-Limited Chemical Reactions, Ph.D. Thesis, California Institute of Technology, and Project SQUID Technical Report CIT-8-PU (December 1976).

MARBLE, F. E. and BROADWELL, J. E. [1977] "The Coherent Flame Model for Turbulent Chemical Reactions", Project SQUID TRW-9-PU.

MUNGAL, M. G. and DIMOTAKIS, P. E. [1984] "Mixing and combustion with low heat release in a turbulent mixing layer", J. Fluid Mech. 148, 349-382.

MUNGAL, M. G. and FRIELER, C. E. [1985] "Chemical reactions in a turbulent mixing layer: The effects of the reaction rate coefficient - Part I", GALCIT report FM85-01 (31-Dec-85).

PAPAMOSCHOU, D. [1986] "Experimental Investigation of Heterogeneous Compressible Shear Layers", Ph. D. thesis, California Institute of Technology.

SMOOKE, M. D., MILLER, J. A. and KEE, R. J. [1983] "Determination of Adiabatic Flame Speeds by Boundary Value Methods", Comb. Sc. & Tech. 34, 79-90.

Appendix: The $H_2/NO/F_2$ chemical system

Chemical equations

1.	$NO + F_2$		$\rightleftharpoons$	$NOF + F$
2.	$NO + F + M$		$\rightleftharpoons$	$NOF + M$
3.	$H + F_2$		$\rightleftharpoons$	$HF + F$
4.	$F + H_2$		$\rightleftharpoons$	$HF + H$
5.	$F_2 + M$		$\rightleftharpoons$	$F + F + M$
6.	$HF + M$		$\rightleftharpoons$	$H + F + M$
7.	$H_2 + M$		$\rightleftharpoons$	$H + H + M$

Rate Coefficients

	A	β	E
1.	4.2×10^{11}	0.0	2285
2.	3.0×10^{16}	0.0	0
3.	3.0×10^{9}	1.5	1680
4.	2.6×10^{12}	0.5	610
5.	2.1×10^{13}	0.0	33700
6.	3.1×10^{13}	0.0	125000
7.	2.2×10^{12}	0.5	92600

These values are derived from Baulch et al [1981] and Cohen et al [1982].